

Nonlinear current-voltage characteristics of oxygen-deficient La_{0.67}Ca_{0.33}MnO₃ films

S. J. Liu, J. Y. Juang, J.-Y. Lin, K. H. Wu, T. M. Uen, and Y. S. Gou

Citation: *Journal of Applied Physics* **103**, 023917 (2008); doi: 10.1063/1.2833433

View online: <http://dx.doi.org/10.1063/1.2833433>

View Table of Contents: <http://scitation.aip.org/content/aip/journal/jap/103/2?ver=pdfcov>

Published by the [AIP Publishing](#)

Articles you may be interested in

[Magnetization reversal mechanism in La_{0.67}Sr_{0.33}MnO₃ thin films on NdGaO₃ substrates](#)

J. Appl. Phys. **107**, 013904 (2010); 10.1063/1.3273409

[Dynamic properties of cluster glass in La_{0.25}Ca_{0.75}MnO₃ nanoparticles](#)

J. Appl. Phys. **106**, 083904 (2009); 10.1063/1.3246869

[Enhanced room temperature magnetoresistance and cluster spin glass behavior in Mo doping La_{0.67}Sr_{0.33}MnO₃](#)

J. Appl. Phys. **105**, 123910 (2009); 10.1063/1.3152600

[Bias-dependent rectifying properties of n-n manganite heterojunctions La_{1-x}Ca_xMnO₃/SrTiO₃:Nb \(x = 0.65 - 1\)](#)

Appl. Phys. Lett. **93**, 212502 (2008); 10.1063/1.3021399

[Oscillatory exchange coupling in La_{0.67}Sr_{0.33}MnO₃/SrTiO₃ superlattices](#)

Appl. Phys. Lett. **91**, 012505 (2007); 10.1063/1.2753707



Re-register for Table of Content Alerts

Create a profile.



Sign up today!



Nonlinear current-voltage characteristics of oxygen-deficient $\text{La}_{0.67}\text{Ca}_{0.33}\text{MnO}_{3-y}$ films

S. J. Liu,^{1(a)} J. Y. Juang,² J.-Y. Lin,³ K. H. Wu,² T. M. Uen,² and Y. S. Gou⁴

¹Department of Materials Engineering, Mingchi University of Technology, Taishan, Taipei 243, Taiwan

²Department of Electrophysics, National Chiao Tung University, Hsinchu 300, Taiwan

³Institute of Physics, National Chiao Tung University, Hsinchu 300, Taiwan

⁴Department of Physics, National Taiwan Normal University, Taipei 106, Taiwan

(Received 17 October 2007; accepted 19 November 2007; published online 25 January 2008)

Two different types of nonlinear current-voltage characteristics are observed in oxygen-deficient $\text{La}_{0.67}\text{Ca}_{0.33}\text{MnO}_{3-y}$ (LCMO) films at temperatures below the insulator-metal transition. The parabolic-like dynamic conductance $G(V)$, defined as dI/dV , curves near the zero bias observed in highly oxygen-deficient LCMO films implies the contribution from the spin-dependent tunneling transport between ferromagnetic clusters, with magnetic-disordered regions serving as tunneling barriers. On the other hand, for the slightly oxygen-deficient LCMO films, dips around the zero bias were observed in nonlinear $G(V)$ curves and have been attributed to spin-flip scattering, with oxygen vacancies serving as scattering centers. © 2008 American Institute of Physics.

[DOI: [10.1063/1.2833433](https://doi.org/10.1063/1.2833433)]

I. INTRODUCTION

The polycrystalline and epitaxial manganite films show different magnetoresistive (MR) behaviors. In epitaxial films and single crystals, large MR is only observed around the insulator-metal transition temperature (T_{IM}) under high magnetic fields. However, for polycrystalline films,^{1,2} ceramics samples,³ and boundary junctions artificially fabricated on bicrystal substrates,^{4,5} large MR is found not only around the T_{IM} but also observed at low temperatures. Moreover, a drastic drop of resistivity is observed at low magnetic fields, followed by a gradual decrease at high magnetic fields. These experimental results led to the extensive studies on the grain-boundary effect that enhances the MR in manganite samples.^{6,7} The low-temperature and low-field MR was tentatively ascribed to the spin-dependent tunneling through an insulating layer separating FM grains with high spin polarization.^{1,7} However, nonlinear electrical conductivity, the most important feature of tunneling behaviors, is found below T_{IM} in boundary junctions deposited on bicrystal substrates^{4,5,8-12} but not always observed in polycrystalline films; both kinds of films exhibit a low-temperature and low-field large MR.⁷ An alternative explanation for the low-field large MR is the spin-dependent scattering occurring at the grain boundaries with magnetic inhomogeneity that serve as scattering centers.² The strength of the scattering centers is field dependent. A strong field orients the magnetic moment within the grain boundaries into a parallel configuration and reduces the scattering.

On the other hand, the strong influence of the oxygen stoichiometry on the crystalline structure and magnetic and transport properties of colossal magnetoresistance (CMR) manganites has been extensively studied.¹³⁻²⁰ In general, oxygen deficiency usually leads to decreases of the ferromagnetic Curie temperature (T_C) and T_{IM} , an increase of

resistivity, a reduction of magnetization, and the manifestation of spin-glass characteristics. However, to the best of our knowledge, until now there has been no literature report on the nonlinear current-voltage ($I-V$) characteristics on oxygen-deficient CMR manganite films. In this work, systematic measurements on magnetization and electrical transport for oxygen-deficient $\text{La}_{0.67}\text{Ca}_{0.33}\text{MnO}_{3-y}$ (LCMO) films have been made to investigate nonlinear $I-V$ characteristics of oxygen-deficient LCMO films.

II. EXPERIMENTAL

The LCMO films used in this work were grown on single-crystalline LaAlO_3 (sample 1209B) and SrTiO_3 (sample 1203A) substrates by pulsed-laser deposition (PLD). Films with different oxygen contents were obtained by controlling the oxygen pressure during PLD. It is well established that a higher oxygen pressure, higher annealing temperature, and longer annealing time during deposition will result in a higher oxygen content in manganite films.¹⁸⁻²⁰ The linear relationship between the T_{IM} and Mn^{4+} content of $\text{La}_{0.67}\text{Ca}_{0.33}\text{MnO}_{3-y}$ films presented by Dörr *et al.*¹⁸ was used to estimate the Mn^{4+} content x and oxygen deficiency y of the films. The detailed preparation conditions and relevant parameters are listed in Table I. The oxygen content of sample 1209B is higher than that of sample 1203A.

The crystalline structure of the as-grown films were examined by x-ray diffraction with $\text{Cu } K\alpha$ radiation. The results showed that the films were all (001)-oriented with excellent epitaxy, and no other secondary or impurity phase was observed (not shown here). The magnetic and transport properties measurements were carried out using a Quantum Design physical property measurement system (PPMS). The resistivities and $I-V$ characteristics of these samples were carried out with a four-probe measurement setup. The

^aElectronic mail: sjliu@mail.mit.edu.tw.

TABLE I. Detailed preparation conditions and parameters of the samples used in this study. T_s and PO_2 is the temperature of substrates and the oxygen pressure during PLD, respectively. T_a is the annealing temperature and t is the annealing time. T_{IM} is the I - M transition temperature in the zero-field $\rho(T)$ curves. T_{SC} is the slope-change temperature (see the text). The x and y are the Mn^{4+} content and oxygen deficiency of the films, respectively.

Samples	T_s (°C)	PO_2 (Torr)	T_a (°C)	t (hour)	T_{IM} (K)	T_{SC} (K)	x	y
1209B	750	0.40	900	0.5	234	...	0.25	0.04
1203A	750	0.25	800	0.5	204	200	0.204	0.063

temperature-dependent resistivity $\rho(T)$ curves were measured by applying a dc constant current of 0.1 mA in the four-probe geometry.

III. RESULTS AND DISCUSSION

The $\rho(T)$ curves are shown in Fig. 1(a). As generally reported, the resistivity evidently increases with increasing oxygen deficiency. T_{IM} is reduced by oxygen deficiency but raised by the application of external fields. Moreover, low-temperature MR implying spin-dependent transport behaviors, similar to that observed in polycrystalline films, is observed in both films and evidently enhanced by the oxygen deficiency. The $M(T)$ curves of samples 1209B and 1203A, as also shown in Fig. 1(a), exhibit no typical PM to FM transition, which is characterized by a sudden increase of magnetization, due to long-range FM coupling, at a specific temperature denoted as T_C . For sample 1209B, an observable onset of magnetization is found around 250 K, which is consistent with the T_{IM} of 234 K obtained from the zero-field $\rho(T)$ curve. However, there is no magnetic crossover or tran-

sition associated with the I - M transition that can be observed in the $M(T)$ curves of sample 1203A. Moreover, the zero-field-cooled (ZFC) and field-cooled (FC) $M(T)$ curves become irreversible below 50 K, indicative of the spin-glass-like characteristics. This can be attributed to the suppression of long-range FM ordering, caused by the reduction of Mn^{4+} - Mn^{3+} pairs.

To further investigate the evolution of magnetic states of oxygen-deficient LCMO films, quantitative analyses were made on the $M(T)$ curves. According to the Curie-Weiss law, $M(T) = C(T - T_C)^{-1}$, with C and T_C being the Curie constant and the Curie temperature, respectively, the magnetization exhibits a reciprocal linear temperature dependence (T^{-1}) when the material is in the PM state. Figure 1(b) shows the $M(T^{-1})$ curve of sample 1203A, showing a linear T^{-1} dependence of magnetization from room temperature down to about 90 K. However, closer inspection reveals a change in the slope of $M(T^{-1})$ curve around 200 K which is consistent with the T_{IM} . It is denoted as the slope-change temperature (T_{SC}) hereafter. The slope change indicates an enhancement of the Curie constant, presumably due to the formation of short-range FM clusters at temperatures below T_{SC} . Nonetheless, the linear temperature dependence of the induced magnetic moments indicates that the FM ordering only takes place inside clusters and the whole system remains in PM state. In other words, the highly oxygen-deficient LCMO films manifest themselves more like in a “superparamagnetic” (SPM) state at temperatures below T_{SC} , rather than transform directly into a long-range-ordered FM state. The absence of long-range FM ordering can be easily related to the oxygen deficiency, since oxygen serves as the bridge between Mn^{3+} and Mn^{4+} in the double-exchange interaction scenario. The temperature-dependent ac susceptibility $\chi_{ac}(T)$ of sample 1203A, as plotted in Fig. 1(c), displays a sharp cusp around 89 K, which is typical for systems exhibiting spin-glass characteristics and evidently identifies the spin-glass-freezing temperature, T_f . For sample 1209B, which is less oxygen deficient than sample 1203A, the $\chi_{ac}(T)$ increases gradually with decreasing temperature and reaches a maximum around 50 K. However, no apparent cusp is observed, consistent with the indiscernible hysteresis between the ZFC and FC $M(T)$ curves, as shown in Fig. 1(a).

The dynamic conductance curves $G(V)$, defined as dI/dV , measured at various temperatures and magnetic fields for samples 1209B and 1203A, are plotted in Figs. 2(a) and 2(b), respectively. It is obvious that the shapes of the zero-field $G(V)$ curves of these two samples are different. For sample 1209B, dips around the zero bias are found. Similar results were reported in bicrystal grain-boundary junctions

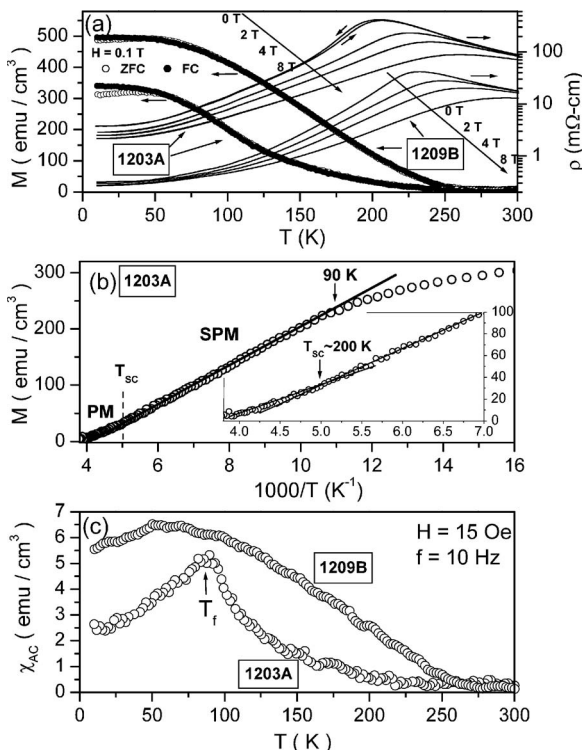


FIG. 1. (a) The temperature dependence of magnetization $M(T)$ and resistivity $\rho(T)$. (b) The evolution of magnetic state with temperature and (c) the temperature-dependent ac susceptibility $\chi_{ac}(T)$ curves of oxygen-deficient $La_{0.67}Ca_{0.33}MnO_{3-y}$ films used in the work.

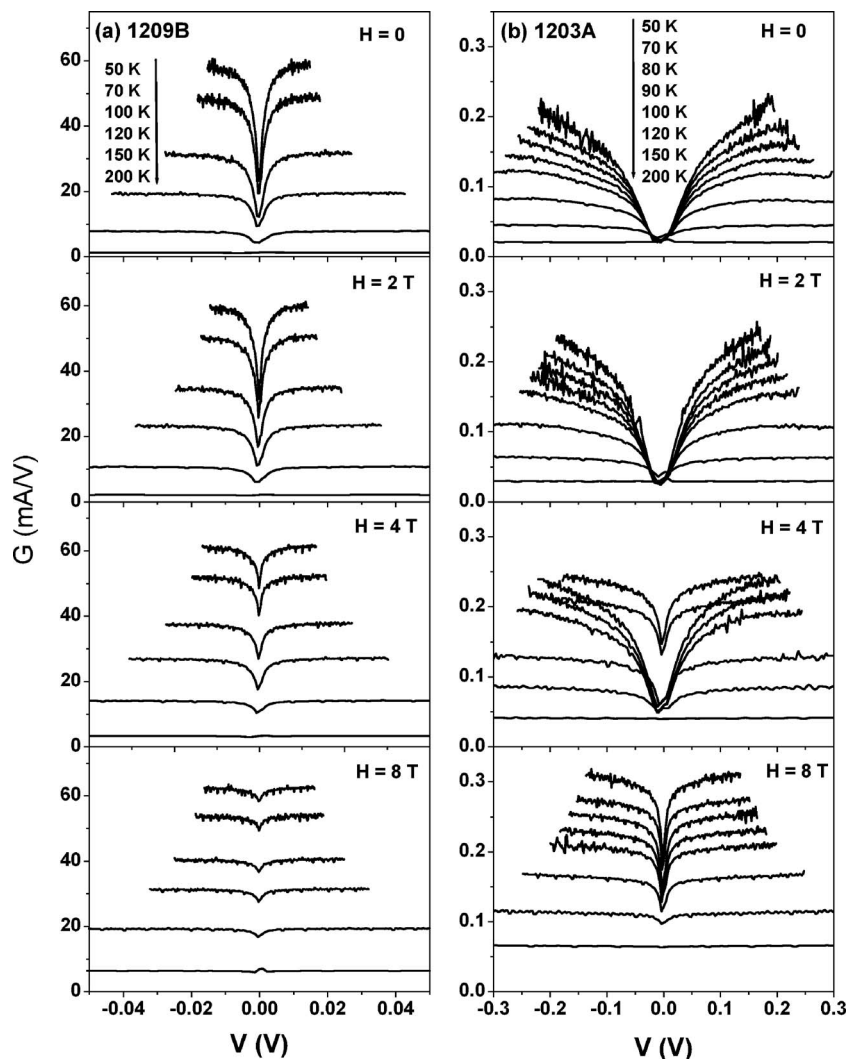


FIG. 2. The dynamic conductance G , defined as dI/dV , measured at various temperatures and magnetic fields for samples (a) 1209B and (b) 1203A.

made of epitaxial $\text{La}_{0.67}\text{Ca}_{0.33}\text{MnO}_3$,⁴ $\text{La}_{2/3}\text{Sr}_{1/3}\text{MnO}_3$,¹⁰ and $\text{La}_{0.6}\text{Pb}_{0.4}\text{MnO}_3$ films,¹² and were attributed to tunneling between FM electrodes separated by the artificial grain boundaries. However, in our case, nonlinearity is only observed in the bias range from -0.02 to $+0.02$ V. This is very different from the previously reported results, whose bias range is several volts. Furthermore, as shown in Fig. 2(a), $G(V)$ increases with decreasing temperature. In other words, the resistance of sample 1209B decreases monotonically with increasing temperature. This is not consistent with tunneling behaviors, which should exhibit an increase in the resistivity with decreasing temperature due to thermally activated or variable range-hopping conduction in the disordered barrier regions.² Moreover, except for oxygen vacancies, no structural disorder exists in the oxygen-deficient LCMO films used in this study. Under a strong field of 8 T, the nonlinearity of the I - V curves of sample 1209B almost vanishes, i.e., the dynamic conductance $G(V)$ is nearly independent of applied voltages.

For sample 1203A, the $G(V)$ curves obtained under zero and 2 T fields are parabolic-like and overlap around the zero bias. However, the shape of the $G(V)$ curves of sample 1203A converts from parabolic-like to a dip when measured under a field of 4 T at temperatures below 70 K. As the

applied field approaches 8 T, the shape of the $G(V)$ curves of sample 1203A is almost the same as that of sample 1209B measured under zero and low fields. The nonlinear behaviors of oxygen-deficient LCMO films depend on the temperature, magnetic field, and oxygen content.

The following scenario is proposed here to explain the present results. In slightly oxygen-deficient films (sample 1209B) the nonlinearity is caused by spin-flip scattering occurring at the oxygen vacancies. Since oxygen is the bridge between Mn ions in the double-exchange mechanism, oxygen vacancies reduce the ferromagnetic coupling. Moreover, the oxygen deficiency reduces the Mn^{3+} and Mn^{4+} pairs; it would result in magnetic inhomogeneity near the vacancies. In other words, it is paramagnetic around the oxygen vacancies. However, ferromagnetic coupling can be enhanced by applying strong external magnetic fields; the scattering height is suppressed by decreasing temperature and strong magnetic fields.

On the other hand, for highly oxygen-deficient films (sample 1203A) the overlap and parabolic-like shape of the zero-field $G(V)$ curves near the zero bias imply the tunneling transport^{21,22} occurring in the magnetic-disordered regions, which are insulating or semiconducting and serve as the tunneling barrier. The magnetic-disordered regions separate the

films into short-range FM clusters and suppress the FM coupling between these clusters, as deduced from the $M(T^{-1})$ characteristics discussed above. Moreover, the barrier height is reduced by magnetic fields. As the magnetic moments in the magnetic-disordered regions are aligned into a parallel configuration by a strong enough magnetic field, the tunneling barriers are eliminated. However, the oxygen vacancies cannot be removed; spin-flip scattering results in the nonlinearity in $G(V)$ curves measured under a strong magnetic field of 8 T.

IV. SUMMARY

In summary, nonlinear $I-V$ characteristics and low-temperature magnetoresistance indicate spin-dependent transport behaviors of oxygen-deficient $\text{La}_{0.67}\text{Ca}_{0.33}\text{MnO}_3$ films. For highly oxygen-deficient films exhibiting superparamagnetic and spin-glass-like characteristics, the spin-dependent tunneling is believed to be responsible for the nonlinear conductance. On the other hand, the nonlinear $I-V$ behaviors observed in slightly oxygen-deficient samples are attributed to spin-flip scattering occurring around the oxygen vacancies.

ACKNOWLEDGMENTS

This work was supported by the National Science Council of Taiwan, under Grant No. NSC 95-2112-M-131-002-MY3.

¹H. Y. Hwang, S.-W. Cheng, N. P. Ong, and B. Batlogg, *Phys. Rev. Lett.* **77**, 2041 (1996).

²X. W. Li, A. Gupta, G. Xiao, and G. Q. Gong, *Appl. Phys. Lett.* **71**, 1124 (1997).

³J. Philip and T. R. N. Kutty, *Appl. Phys. Lett.* **79**, 79 (2001).

⁴W. Westerburg, F. Martin, S. Friedrich, M. Maier, and G. Jakob, *J. Appl. Phys.* **86**, 2173 (1999).

⁵N. Khare, U. P. Moharil, A. K. Gupta, A. K. Raychaudhuri, S. P. Pai, and R. Pinto, *Appl. Phys. Lett.* **81**, 325 (2002).

⁶J. E. Evetts, M. G. Blamire, N. D. Mathur, S. P. Isaac, B. S. T. L. F. Cohen, and J. L. Macmanus-Driscoll, *Philos. Trans. R. Soc. London, Ser. A* **356**, 1593 (1998).

⁷M. Ziese, *Phys. Rev. B* **60**, R738 (1999).

⁸N. K. Todd, N. D. Mathur, S. P. Isaac, J. E. Evetts, and M. G. Blamire, *J. Appl. Phys.* **85**, 7263 (1999).

⁹R. Gross, L. Alff, B. Buchner, B. H. Freitag, C. Höfener, J. Klein, Y. Lu, W. Mader, J. B. Philipp, M. S. R. Rao, P. Reutler, S. Ritter, S. Thienhaus, S. Uhlenbruck, and B. Wiedenhorst, *J. Magn. Magn. Mater.* **211**, 150 (2000).

¹⁰R. Gunnarsson, A. Kadigrobov, and Z. Ivanov, *Phys. Rev. B* **66**, 024404 (2002).

¹¹M. Paranjape, J. Mitra, A. K. Raychaudhuri, N. K. Todd, N. D. Mathur, and M. G. Blamire, *Phys. Rev. B* **68**, 144409 (2003).

¹²P. Chowdhury, S. K. Gupta, N. Padma, C. S. Viswanadham, S. Kumar, A. Singh, and J. V. Yakhmi, *Phys. Rev. B* **73**, 104437 (2006).

¹³H. L. Ju, J. Gopalakrishnan, J. L. Peng, Q. Li, G. C. Xiong, T. Venkatesan, and R. L. Greene, *Phys. Rev. B* **51**, 6143 (1995).

¹⁴C. Ritter, M. R. Ibarra, J. M. D. Teresa, P. A. Algarabel, C. Marquina, J. Blasco, J. Garcia, S. Oseroff, and S.-W. Cheong, *Phys. Rev. B* **56**, 8902 (1997).

¹⁵Z. L. Wang, J. S. Yin, Y. D. Jiang, and J. Zhang, *Appl. Phys. Lett.* **70**, 3362 (1997).

¹⁶N. Malde, P. S. I. P. N. de Silva, A. K. M. A. Hossian, L. F. Cohen, K. A. Thomas, J. L. MacManus-Driscoll, N. D. Mathur, and M. G. Blamire, *Solid State Commun.* **105**, 643 (1998).

¹⁷J. Li, C. K. Ong, J.-M. Liu, Q. Huang, and S. J. Wang, *Appl. Phys. Lett.* **76**, 1051 (2000).

¹⁸K. Dörr, J. M. D. Teresa, K.-H. Müller, D. Eckert, T. Walter, E. Vlahov, K. Nenkov, and L. Schultz, *J. Phys.: Condens. Matter* **12**, 7099 (2000).

¹⁹R. Cauro, A. Gilabert, J. P. Contour, R. Lyonnet, M.-G. Medici, J.-C. Grenet, C. Leighton, and I. K. Schuller, *Phys. Rev. B* **63**, 174423 (2001).

²⁰X. F. Song, G. J. Lian, and G. C. Xiong, *Phys. Rev. B* **71**, 214427 (2005).

²¹J. G. Simmons, *J. Appl. Phys.* **34**, 1793 (1963).

²²J. G. Simmons, *J. Appl. Phys.* **35**, 2655 (1964).